# Interorbital pair scattering in two-band superconductors

Anna Ciechan and Karol Izydor Wysokiński*
*Institute of Physics and Nanotechnology Centre, M. Curie-Skłodowska University, ul. Radziszewskiego 10, Pl 20-031 Lublin, Poland*
(Received 4 September 2009; revised manuscript received 1 December 2009; published 23 December 2009)

The calculations of local and global properties of two-band superconductors have been presented with particular attention paid to the role of the interorbital scattering of pairs. The properties of such superconductors are very different from a single-band or typical two-band systems with dominant intraband pairing interactions. The effect of the Van Hove singularity in one of the bands on the properties of the intraband clean superconductor has been discussed. It leads to marked increase in superconducting transition temperature in the weak-coupling limit. We also study the inhomogeneous systems in which characteristics change from place to place by solving the Bogolubov-de Gennes equations for small clusters. Suppression of the superconducting order parameter by the single impurity scattering fermions between two orbitals is contrasted with that due to intraorbital impurity scattering. The results obtained for impure systems have been shown as maps of local density of states, order parameter, and gap function. They can be directly compared with the scanning tunneling microscope spectra of real material.

DOI: 10.1103/PhysRevB.80.224523 PACS number(s): 71.10.Fd, 74.20.−z, 74.81.−g

## I. INTRODUCTION

Already in 1950s and 1960s of the last century the main properties of the two-band superconductors have been clarified.[1–4] At that time, however, existing materials did not show clear evidence of two-band behavior. The experimental situation has changed with the discovery of high-temperature superconducting oxides[5] and even more with subsequent discoveries of strontium ruthenate,[6] magnesium diboride,[7] and iron pnictides.[8,9] Even though all of these systems have a number of bands in the vicinity of the Fermi energy, their presence shows up in a different way.

Magnesium diboride clearly shows two different gaps of the same symmetry.[10,11] In strontium ruthenate the three-band model seems to be necessary to explain its puzzling properties.[12,13] The model of superconductivity in iron pnictides is a matter of the ongoing debate.[14–17] Iron pnictides possess a large number of bands around the Fermi energy and a few of them seem to play an important role in the superconducting state.[18–20] A two-band model has been proposed as a minimal one for these superconductors.[21]

With two bands near the Fermi energy one generally expects formation of intraband and interband pairs. In the latter case the pairs have in general nonzero center of mass momentum.[22] The simpler case[1] of superconductivity with the intraband pairs, which can be scattered between two bands seems to be relevant in modeling of pnictides. Indeed, there are strong theoretical[23,24] arguments that the interband interactions may be important in iron superconductors. These findings make pnictides rather different from $MgB_2$ in which a main coupling mechanism is of intraband character.[25] Thus, the detailed study of the interband[26] pair-scattering mechanism of superconductivity is timely and of importance. Recently this issue has been discussed in connection with both cuprate[27] and pnictide superconductors.[28]

In this paper, we focus on both clean and disordered two-band superconductors. In the clean homogeneous systems the wave vector is a good quantum number and energy bands in $k$ space are well defined. On the other hand, the model of impure system is more naturally and precisely formulated in terms of orbitals in real space. Thus we will use the band picture when discussing clean homogeneous systems and real-space representation (sites and orbitals) as far as impure materials are concerned.

We are mainly interested in the interorbital only mechanism of superconductivity. Without loss of generality we denote two orbitals as 1 and 2. The interaction $U_{11}$ ($U_{22}$) is responsible for superconducting instability inside a band formed by orbitals 1 (2), whereas $U_{12}$ promotes scattering of the superconducting pairs between orbitals 1 and 2. The impurity scattering potential is assumed to be short ranged and of the general form $\sim V_{imp}^{\lambda\lambda'} c_{i\lambda\sigma}^{+} c_{i\lambda'\sigma}$. It scatters electrons from site $i$, orbital $\lambda'$ into orbital $\lambda$ of the same site. If $\lambda=\lambda'$ we call such impurities intraorbital, if $\lambda\neq\lambda'$ interorbital.

The organization of the rest of the paper is as follows. Section II presents the general Hamiltonian of the two-orbital model and the Bogolubov-de Gennes (BdG) approach used to solve it. Homogeneous superconductors are discussed in Sec. III, where we study *inter alia* the effect of the Van Hove singularity in the density of states in one of the bands on the properties of the superconductors with interband pair scattering only. The changes induced in the superconductor by single intraorbital or interorbital impurities are discussed in Sec. IV, whereas the finite concentration of impurities is considered in Sec. V. We end up with the discussion of our results and their relevance to the most prominent two-band superconductors: $MgB_2$ and iron pnictides.

## II. HAMILTONIAN FOR THE TWO-ORBITAL SUPERCONDUCTOR

We start with a general Hamiltonian in a real space describing the system with two orbitals. We assume the spin-independent effective pairing interaction between fermions in various orbital states. The randomness in the system is easily incorporated *via* site dependence of parameters. The Hamiltonian reads

 

$$H = \sum_{ij,\lambda\lambda',\sigma} [-t_{ij}^{\lambda\lambda'} + V_{imp}^{\lambda\lambda'}(\vec{r}_i)\delta_{ij}]c_{i\lambda\sigma}^{+}c_{j\lambda'\sigma} + \sum_{i,\lambda,\sigma} (e_\lambda - \mu)c_{i\lambda\sigma}^{+}c_{i\lambda\sigma} + \sum_{i,\lambda_1\lambda_2,\lambda_3\lambda_4} U_{\lambda_1\lambda_2\lambda_3\lambda_4}(\vec{r}_i)c_{i\lambda_1\uparrow}^{+}c_{i\lambda_2\downarrow}^{+}c_{i\lambda_3\downarrow}c_{i\lambda_4\uparrow}, \quad (1)$$

where $c_{i\lambda\sigma}^{+}$, $c_{i\lambda\sigma}$ are the creation and annihilation operators of electrons with spin $\sigma=\uparrow,\downarrow$ at the lattice site $\vec{r}_i=i$ in the orbital $\lambda$. $\epsilon_\lambda$ is the electron energy and $\mu$ is the chemical potential. $t_{ij}^{\lambda\lambda'}$ are the hopping integrals between the same or different orbitals (if $\lambda\neq\lambda'$). $U_{\lambda_1\lambda_2\lambda_3\lambda_4}(\vec{r}_i)$ denotes the interactions, which are attractive if $U_{\lambda_1\lambda_2\lambda_3\lambda_4}(\vec{r}_i)<0$. The dependence of the interaction parameters on the position $\vec{r}_i$ allows to treat systems with inhomogeneous pairing.

We use the standard mean-field decoupling valid for a spin-singlet superconductor and get the effective Hamiltonian

$$H^{MFA} = \sum_{ij,\lambda\lambda',\sigma} [-t_{ij}^{\lambda\lambda'} + V_{imp}^{\lambda\lambda'}(\vec{r}_i)\delta_{ij}]c_{i\lambda\sigma}^{+}c_{j\lambda'\sigma} + \sum_{i,\lambda,\sigma} [\epsilon_\lambda + V_{\lambda,\sigma}(\vec{r}_i) - \mu]c_{i\lambda\sigma}^{+}c_{i\lambda\sigma} + \sum_{i,\lambda\lambda'} [\Delta_{\lambda\lambda'}(\vec{r}_i)c_{i\lambda\uparrow}^{+}c_{i\lambda'\downarrow}^{+} + \text{H.c.}], \quad (2)$$

where the order parameters $\Delta_{\lambda\lambda'}(\vec{r}_i)$ are related to the pairing correlation functions $f_{\lambda\lambda'}(\vec{r}_i)=\langle c_{i\lambda\downarrow}c_{i\lambda'\uparrow}\rangle$ through

$$\Delta_{\lambda_1\lambda_2}(\vec{r}_i) = -\sum_{\lambda_3\lambda_4} U_{\lambda_1\lambda_2\lambda_3\lambda_4}(\vec{r}_i)f_{\lambda_3\lambda_4}(\vec{r}_i). \quad (3)$$

The local Hartree terms $V_\lambda(\vec{r}_i)$ depend on the number of particles at a given site $n_{\lambda\sigma}(\vec{r}_i)=\langle c_{i\lambda\sigma}^{+}c_{i\lambda\sigma}\rangle$

$$V_{\lambda\sigma}(\vec{r}_i) = \sum_{\lambda'} U_{\lambda'\lambda\lambda'}(\vec{r}_i)n_{\lambda'-\sigma}(\vec{r}_i). \quad (4)$$

We consider here only the diagonal correlations $\langle c_{i\lambda\sigma}^{+}c_{i\lambda'\sigma'}\rangle = \delta_{\lambda\lambda'}\delta_{\sigma\sigma'}n_{\lambda\sigma}(\vec{r}_i)$.

Hamiltonian (2) is diagonalized using the Bogolubov-Valatin transformation[29,30]

$$c_{i\lambda\uparrow} = \sum_\nu [u_{\lambda\nu}(\vec{r}_i)\gamma_{\nu\uparrow} - v_{\lambda\nu}^{*}(\vec{r}_i)\gamma_{\nu\downarrow}^{+}], \quad (5)$$

$$c_{i\lambda\downarrow} = \sum_\nu [u_{\lambda\nu}(\vec{r}_i)\gamma_{\nu\downarrow} + v_{\lambda\nu}^{*}(\vec{r}_i)\gamma_{\nu\uparrow}^{+}] \quad (6)$$

leading to the BdG equations for the amplitudes $u_{\lambda\nu}(\vec{r}_i)$, $v_{\lambda\nu}(\vec{r}_i)$ and the eigenenergies $E_\nu$

$$\sum_{j,\lambda'} K_{ij}^{\lambda\lambda'}u_{\lambda'\nu}(r_j) + \sum_{\lambda'} \Delta_{\lambda\lambda'}(\vec{r}_i)v_{\lambda'\nu}(\vec{r}_i) = E_\nu u_{\lambda\nu}(\vec{r}_i), \quad (7)$$

$$-\sum_{j,\lambda'} K_{ij}^{\lambda\lambda'}v_{\lambda'\nu}(r_j) + \sum_{\lambda'} \Delta_{\lambda\lambda'}^{*}(\vec{r}_i)u_{\lambda'\nu}(\vec{r}_i) = E_\nu v_{\lambda\nu}(\vec{r}_i), \quad (8)$$

where the operator $K_{ij}^{\lambda\lambda'}$ reads

$$K_{ij}^{\lambda\lambda'} = [e_\lambda - \mu + V_{\lambda\sigma}(\vec{r}_i)]\delta_{ij}\delta_{\lambda\lambda'} + V_{imp}^{\lambda\lambda'}(\vec{r}_i)\delta_{ij} - t_{ij}^{\lambda\lambda'}. \quad (9)$$

The pairing parameters $\Delta_{\lambda\lambda'}(\vec{r}_i)$ and the Hartree potentials $V_\lambda(\vec{r}_i)$ are, in turn, expressed in terms of the eigenfunctions and eigenergies $u_{\lambda\nu}(\vec{r}_i)$, $v_{\lambda\nu}(\vec{r}_i)$, $E_\nu$ as[31]

$$n_\lambda(\vec{r}_i) = \sum_\nu [|u_{\lambda\nu}(\vec{r}_i)|^2 f_\nu + |v_{\lambda\nu}(\vec{r}_i)|^2(1-f_\nu)], \quad (10)$$

$$f_{\lambda\lambda'}(\vec{r}_i) = \sum_\nu [u_{\lambda\nu}(\vec{r}_i)v_{\lambda'\nu}^{*}(\vec{r}_i)(1-f_\nu) - u_{\lambda'\nu}(\vec{r}_i)v_{\lambda\nu}^{*}(\vec{r}_i)f_\nu]. \quad (11)$$

In the above formulae $f_\nu=(e^{E_\nu/k_BT}+1)^{-1}$ denotes the Fermi-Dirac distribution function of quasiparticles. The total number of particles is given by $n=\Sigma_\lambda N_\lambda/L=\Sigma_{i\lambda}n_\lambda(\vec{r}_i)/L$, where $L$ is a number of sites in the cluster.

The local density of states (DOS) $N(\vec{r}_i,E)$ is directly accessible in scanning tunneling microscope (STM) measurements and is proportional to the local conductance $dI(\vec{r}_i,V)/dV$. In the two-orbital system it is a sum of local densities of states $N(\lambda,\vec{r}_i,E)$

$$N(\lambda,\vec{r}_i,E) = \sum_\nu [|u_{\nu\lambda}(\vec{r}_i)|^2\delta(E-E_\nu) + |v_{\nu\lambda}(\vec{r}_i)|^2\delta(E+E_\nu)]. \quad (12)$$

Obviously, we have in each site $N(\vec{r}_i,E)=N(1,\vec{r}_i,E)+N(2,\vec{r}_i,E)$. For a clean system Eqs. (7) and (8) can be Fourier transformed and written (in an analogous form) in reciprocal space. For the impure systems with broken translational symmetry, the Bogolubov-de Gennes Eqs. (7) and (8) are solved self-consistently in the real space for a small $n\times m$ cluster with periodic boundary conditions. For a two-orbital model the typical size of the cluster is $20\times30$. In the next section we start with the comparison of our real-space (for small cluster) calculations with the numerically exact results obtained in the reciprocal space (i.e., for bulk system).

## III. HOMOGENEOUS SUPERCONDUCTORS

In this section we discuss some properties of homogeneous two-band superconductors paying a special attention to the comparison of the accuracy of small cluster calculations with those for the bulk system. We also consider the effect of the Van Hove singularity in one of the bands on properties of interband pairing superconductivity and the role of various interband couplings.

### A. Small clusters vs. bulk systems

We start with the homogeneous system with two orbitals denoted as 1 and 2. The superconductor is described by the following set of parameters. The interorbital interaction[1] has the form of pair scattering only $U_{12}=U_{1122}$, whereas the two intraorbital interactions are $U_{11}=U_{1111}$ and $U_{22}=U_{2222}$. We consider a two-dimensional square lattice with nonzero hopping integrals between the nearest-neighbor sites only $t_\lambda$

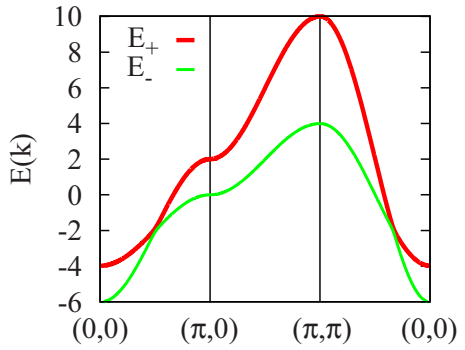


FIG. 1. (Color online) Energy bands of the two-dimensional square lattice with the parameters $e_2-e_1=2t$, $t_1=t$, $t_2=2t$, and $t_{12}=0.05t$. The chemical potential is located at $\mu=0$ and the resulting total number of particles $n=1.62$.

$=t_{ij}^{\lambda\lambda}$ and hybridization $t_{12}=t_{ij}^{12}$. We set the direct hoping between orbitals no. 1 as our energy unit $t_1=t=1$. Since we neglect the possibility of interorbital pairs, we use the simpler notation $\Delta_1=\Delta_{11}$ and $\Delta_2=\Delta_{22}$.

Figure 1 shows the single-particle energy bands along main symmetry directions in the two-dimensional Brillouin zone obtained for the set of parameters $e_2-e_1=2t$, $t_1=t$, $t_2=2t$, and $t_{12}=0.05t$. The chemical potential $\mu=0$ and the total number of carriers $n=1.62$.

Figure 2 compares the solutions obtained for the bulk system with those for small clusters of various sizes. We consider here the bulk data accurate as determination of the gap parameter for the bulk homogeneous system (in our case

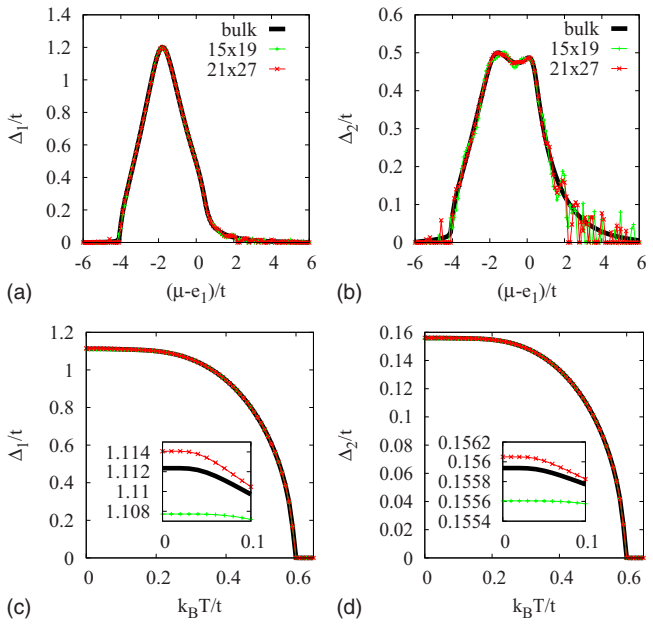


FIG. 2. (Color online) The upper panels show the dependence of $\Delta_\lambda$ for both bands on the chemical potential $\mu$ for the bulk system (solid curve) and for the clusters of size $15\times19$ (thin line with pluses) and $21\times27$ (line with crosses). The other parameters are: $e_2-e_1=2t$, $t_1=t$, $t_2=2t$, $t_{12}=0.05t$, $U_1=-3.5t$, $U_2=-3t$, and $U_{12}=-0.5t$. At the lower panels temperature dependences of $\Delta_\lambda$ are shown for $e_1-\mu=2t$. The insets show the data near $T=0$ on the expanded scale.

assumed to be on the order of $10^{-6}t$) is only limited by the time of calculations. We have found that at the band center the results obtained for the clusters with the size as great as 400 sites are acceptable. Relative changes in the gaps with respect to the bulk values

$$\delta\Delta_\lambda = [\Delta_\lambda(L) - \Delta_\lambda^{bulk}]/\Delta_\lambda^{bulk} \cdot 100\%$$

are in the range of $\delta\Delta_1<0.15\%$ in the first band and slightly larger $\delta\Delta_2<1.5\%$ for the second band. Well inside the bands the spectrum is quasicontinuous and the results agree very well with the bulk data but near the band edges the spectrum of finite clusters is discrete and the differences are greater (cf. Fig. 2).

### B. Interband pairing only superconductor—The role of Van Hove singularity

Here we treat a homogeneous superconductor with two bands and the interaction scattering the pairs between them.[1] The symbol $\lambda$ is used here to denote the band in $\vec{k}$ space.

As a general rule, one finds that the interband scattering $U_{12}$ plays a minor role in superconductors with dominant intraband interactions.[32] This interaction, however couples two bands and may lead to the increase in the superconducting transition temperature.[4,33] The situation changes drastically if the interband pairing is the only existing interaction. The properties of the superconductors with dominant interband scattering are markedly different from those with dominant intraband interactions. In particular,[34] the superconducting transition takes place for an arbitrary sign of $U_{12}$. The value of the gap in the first band is determined by the interaction $U_{12}$ and the density of states in the second band and vice versa, the gap in the second band is proportional to the partial DOS at the Fermi level in the first band.

This can be easily seen from the general two-band BCS equations[1]

$$\Delta_1(1+U_{11}F_1) = -U_{12}\Delta_2F_2,$$

$$\Delta_2(1+U_{22}F_2) = -U_{12}\Delta_1F_1, \tag{13}$$

where

$$F_\lambda = \int_0^{\hbar\omega_c} dE N_\lambda(E) \frac{\tanh\dfrac{\sqrt{E^2+\Delta_\lambda^2}}{2k_BT}}{\sqrt{E^2+\Delta_\lambda^2}} \tag{14}$$

and $N_\lambda(E)$ denotes single-particle density of states in the band $\lambda$. As we are interested in the limit of interband pair scattering only we put $U_{11}=U_{22}=0$. The above equations reduce to

$$\Delta_1 = -U_{12}\Delta_2 \int_0^{\hbar\omega_c} dE N_2(E) \frac{\tanh\dfrac{\sqrt{E^2+\Delta_2^2}}{2k_BT}}{\sqrt{E^2+\Delta_2^2}},$$

$$\Delta_2 = -U_{12}\Delta_1 \int_0^{\hbar\omega_c} dE N_1(E) \frac{\tanh\frac{\sqrt{E^2+\Delta_1^2}}{2k_BT}}{\sqrt{E^2+\Delta_1^2}}. \quad (15)$$

It is clear from Eq. (15) that the value of $\Delta$ in the second band is determined by the density of states in the first one and vice versa. It is also obvious that nonzero solutions can be obtained for both signs and an arbitrarily small value of the coupling $U_{12}$. For its positive value the order parameters in the two bands have opposite signs, whereas for negative $U_{12}$ they are of the same sign.

The model with interorbital pairing only has a number of unusual features. It has been found[28,35] that the ratio $\Delta_2/\Delta_1 = \sqrt{N_1/N_2}$, where $N_2(N_1)$ is the density of states at the Fermi level in band 2(1). The superconducting transition temperature of the system is given by the BCS-type expression

$$T_c = 1.136\frac{\hbar\omega_c}{k_B}\exp\left(\frac{-1}{\lambda_{eff}}\right) \quad (16)$$

with $\lambda_{eff}=\lambda_0=\sqrt{U_{12}^2 N_1 N_2}$. The dependence of $\lambda_{eff}$ on the square of $U_{12}$ shows that superconducting transition temperature is the same independent whether the interaction is attractive or repulsive.

It often happens that the Fermi level in superconductors lies close to the Van Hove singularity. In the layered systems with nesting properties of the (quasi-two-dimensional) Fermi surface, the density of states near the Van Hove singularity changes logarithmically

$$N(E) = N_0 \ln(2W/|E|)\Theta(|E|-W), \quad (17)$$

with $2W$ being the bandwidth and $\Theta(x)$ the step function. It is known that the existence of such singularity modifies[36] the BCS expression for the transition temperature, Eq. (16). In particular, in the one-band case and the weak-coupling limit[37] $\lambda \ll 1$, it leads to the increase in superconducting transition by changing the effective interaction: $\frac{1}{\lambda_{eff}} = \sqrt{\frac{2}{\lambda_0}}$.

Here we assume the density of states in the second band to be singular $N(2,E)=N_2 \ln(2W/|E|)$ near the Fermi energy, whereas that of the first band as flat $N(1,E)=N_1$. Near $T_c$ Eq. (15) are linearized, we approximate $\tanh(x)=min(x,1)$ and find (we put here $\hbar=k_B=1$)

$$\Delta_1 = -\Delta_2 U_{12} N_2 \left[1 + \ln\frac{2W}{\omega_c} + \ln\frac{\omega_c}{2T_c} + \ln\frac{2W}{\omega_c}\ln\frac{\omega_c}{2T_c} + \frac{1}{2}\left(\ln\frac{\omega_c}{2T_c}\right)^2\right],$$

$$\Delta_2 = -\Delta_1 U_{12} N_1 \left[1 + \ln\frac{\omega_c}{2T_c}\right]. \quad (18)$$

The analysis of the above set of equations in the weak-coupling limit ($U_{12}\to 0$) leads to the approximate BCS-type expression (16) for the superconducting transition temperature with $\frac{1}{\lambda_{eff}} = \frac{2^{1/3}}{\lambda_0^{2/3}} = \left(\frac{2}{U_{12}^2 N_1 N_2}\right)^{1/3}$ and to the modification of the prefactor, which changes from $1.136\omega_c$ to $1.136\omega_c(2W/\omega_c)^{2/3}$. It is interesting to note that up to the prefactor the Van Hove singularity in one of the bands increases $T_c$ of the intraband superconductor at the weak coupling only $\lambda_0 \le 0.5$.

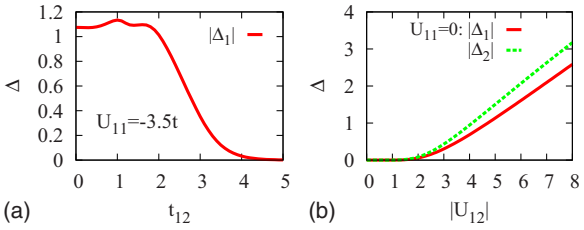


FIG. 3. (Color online) Increase in the hybridization results in significant decrease in $\Delta_1$ for $t_{12}>2$ (left panel). For a given set of parameters ($e_2-e_1=2t$, $t_1=t$, $t_2=2t$, $U_{11}=-3.5t$, $n=1.2$), it is mainly due to diminishing the density of states near the Fermi energy (cf. Fig. 4). Right panel shows the dependence of both order parameters on the modulus of the intraorbital interaction $U_{12}$ in a model with $t_{12}=0$ and $U_{11}=U_{22}=0$.

In a similar way one can calculate the effect of the Van Hove singularity on the ratio of the gaps $\frac{\Delta_2}{\Delta_1}$ at zero temperature. One finds

$$\Delta_1(0) = -\Delta_2(0) U_{12} N_2 \left\{1 - \ln\frac{\Delta_2(0)}{2W} - \frac{1}{2}\left(\ln\frac{\omega_c}{2W}\right)^2 + \frac{1}{2}\left[\ln\frac{\Delta_2(0)}{2W}\right]^2\right\},$$

$$\Delta_2(0) = -\Delta_1(0) U_{12} N_1 \ln\frac{2\omega_c}{\Delta_1(0)}. \quad (19)$$

Even in the extreme weak-coupling limit $\lambda_0\to 0$ when $T_c$, $\Delta_1$, and $\Delta_2\to 0$ the gap ratio is not given by that of the densities of states and depends on $T_c$ and thus $\lambda_0$. The ratio $\frac{\Delta_1}{\Delta_2}$ decreases from the value much larger than $\sqrt{\frac{N_2}{N_1}}$ for small $\lambda_0$ to the values well below $\sqrt{\frac{N_2}{N_1}}$ for larger $\lambda_0$. However, it is interesting to note that the correct description of the intraband superconductivity requires the strong-coupling theory,[28] even if $\lambda_0<1$. The Van Hove singularity plays a similar role in the Eliashberg theory.[36]

### C. The role of the band couplings

Before the presentation of real-space local properties of the model with general interactions we further discuss the homogeneous systems and the influence of model parameters on the superconducting bulk state. In particular, we are interested in the dependence of superconducting state on the couplings between orbitals. The hybridization parameter $t_{12}$ provides single-particle coupling and the interband pair scattering $U_{12}$ provides the direct two-body interorbital interaction. The hybridization changes a single-particle spectrum and this influences the superconductivity.

Figure 3 (left panel) shows the changes in the order parameter $\Delta_1$ due to the increase in the hybridization $t_{12}$. The strong decrease in $\Delta_1$ with $t_{12}$ results from the changes in the single-particle spectrum in the bands. One observes decrease in the projected density of states around the Fermi level. This

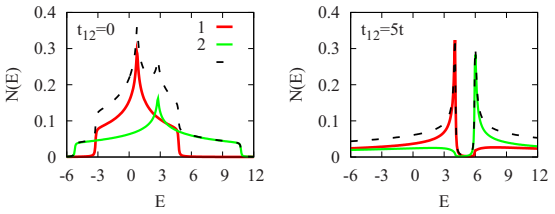


FIG. 4. (Color online) Changes in the normal-state density of states (total—the dashed curve; projected onto respective orbitals, solid curves) for the system as in Fig. 3 with the hybridization $t_{12}=0$ (left panel) and $5t$ (right panel). The Fermi energy is at $E=0$.

is illustrated in Fig. 4. Left panel shows the total (dashed curve) and projected onto orbital 1 and 2 densities of states in the system without any interband coupling ($t_{12}=0$), whereas in the right panel for strong hybridization $t_{12}=5t$. It is worth mentioning that the existence of nonvanishing hybridization $t_{12}$ between the orbitals is sufficient to induce the pairing field $\langle c_{i2\downarrow}c_{i2\uparrow}\rangle$ even if $U_{22}=U_{12}=0$.

As mentioned, the interorbital interaction alone (no hybridization) leads to the superconducting instability independently if it is repulsive or attractive. It induces gaps in both bands. The results are shown in the right panel of Fig. 3. The value of the gap in the *second band* is larger because the density of states near $E_F$ *in the first band* is larger [cf. Eq. (15)]. The simultaneous presence of the interband ($U_{12}$) and intraband (here $U_{11}$ only) interactions results in the increase in the order parameter in the active band, the appearance of $\Delta$ in the nonactive band and characteristic modifications of the quasiparticle density of states as illustrated in Fig. 5. The nonzero density of states around chemical potential for $U_{12}=0$ is simply a result of the absence of couplings between the bands (as also $t_{12}=0$) and the lack of pairing in the second band. This presents the (slightly artificial) case of coexisting normal electrons and coherent Cooper pairs in the system.

This ends up our analysis of the homogeneous two-band superconductors. In the next sections we study various inhomogeneities starting with single potential scatterer.

## IV. SINGLE POTENTIAL IMPURITY IN A CLEAN SUPERCONDUCTOR

In this section we study a single short-ranged nonmagnetic impurity embedded in an otherwise clean system. We

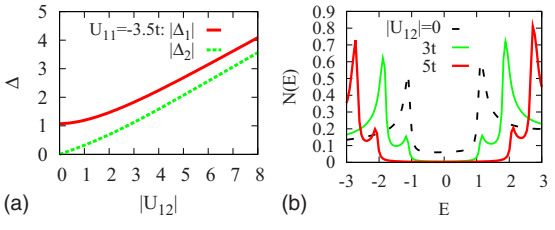


FIG. 5. (Color online) The dependence of $\Delta_1$ and $\Delta_2$ on $U_{12}$ in the superconductor with the intraband attraction $U_{11}=-3.5t$ (left panel). The right panel shows the energy dependence of the quasiparticle density of states for a few values of the interband interaction between bare bands ($t_{12}=0$). The structure in the quasiparticle DOS is due to the gap induced in the nonactive band.

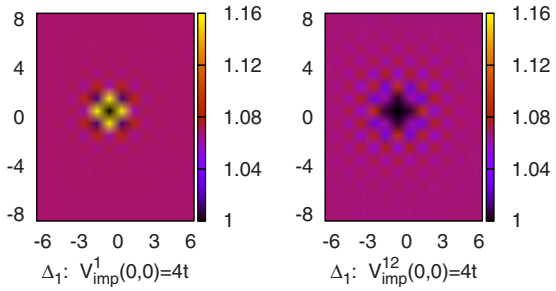


FIG. 6. (Color online) The influence of intraorbital impurity $V^1_{imp}(\vec{r}_i)$ (left panel) and interorbital $V^{12}_{imp}(\vec{r}_i)$ (right panel) impurity of the same strength ($=4t$) on the local values of $\Delta_1(\vec{r}_i)$ in a superconductor with $U_{11}=-3.5t$ and $U_{12}=0$.

solve BdG Eqs. (7) and (8) on a small cluster of the size $L=13\times17$ with an impurity placed in its center. In the two-orbital model the impurity may scatter electrons from a given orbital to the same orbital (intraorbital scattering denoted $V^{1(2)}_{imp}$) or to the other orbital (interorbital scattering—$V^{12}_{imp}$) located at the same site. We allow for both, the intraorbital and interorbital pairing interactions and compare the $T_c$ changes induced by two types of impurities. We are using Bogolubov-de Gennes approach which allows for the distortion of the wave function around impurity and is more suitable to treat inhomogeneous superconductors than the BCS or Eliashberg (both $\vec{k}$-space-based) theories.[31]

We consider the system described by the following set of parameters $e_2-e_1=2t$, $t_1=t$, $t_2=2t$, $t_{12}=0.05$, and $n=1.2$, and start with the pairing interaction between electrons occupying the first orbital only: $U_{11}\neq0$ and $U_{12}=0$. Due to the weak hybridization $t_{12}=0.05t$ there exists small coupling between the bare bands. Figure 6 illustrates the changes in the order parameter $\Delta_1$ around intraorbital (left panel) and interorbital (right panel) impurities. Note different patterns of changes in $\Delta_1$. The intraorbital impurity more strongly suppresses the order parameter at the impurity site and leads to its slight increase at nearest-neighbor sites with respect to the value for the homogeneous system. On the other hand the interorbital impurity scattering diminishes the order parameter at the impurity site and around it but slightly less for the next-nearest neighbors than for the nearest neighbors. The interorbital impurity modifies the order parameter at the distances larger than the intraorbital one, even if both impurities are of the on-site variety. For the parameters used we find $\Delta_1=1.07t$ for the clean system. At the impurity site one finds the strongly suppressed values: $\Delta_1(0,0)=0.17t$ for $V_{imp}(\vec{r}_i)=V^{12}_{imp}(\vec{r}_i)$ and $\Delta_1(0,0)=0.11t$ for $V_{imp}(\vec{r}_i)=V^1_{imp}(\vec{r}_i)=4t$.

In Fig. 7 we show the local quasiparticle density of states at the impurity site $\vec{r}=(0,0)$ and its nearest (0,1) and next-nearest (1,1) neighbor sites. The interorbital impurity induces states inside the gap.

The interesting aspect of these studies is connected with the fact that the effect of $V^{12}_{imp}$ depends on the sign of the interorbital interaction $U_{12}$. There is no similar dependence connected with intraorbital impurities ($V^1_{imp}$ or $V^2_{imp}$). This is illustrated in Fig. 8. The changes in the order parameters $\Delta_1$ and $\Delta_2$ clearly depend on the sign of interorbital interaction. For the clean system we have $|\Delta^0_1|=2.69t$, $|\Delta^0_2|=2.07t$. At the

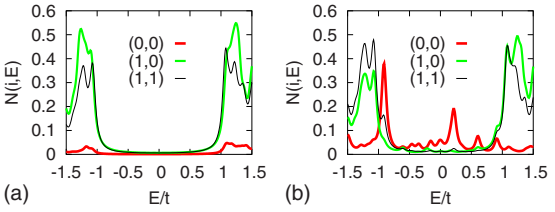


FIG. 7. (Color online) The energy dependence of the local quasiparticle density of states projected onto orbital 1, at the impurity site (0,0) and its neighbors for the system with intraband (left panel) and interband (right panel) impurities for $U_{11}=-3.5t$ and $U_{12}=0$.

interorbital impurity site we find $|\Delta_1|=1.61t$ and $|\Delta_2|=1.21t$ for $U_{12}=-5t$, i.e., roughly 40% reduction. On the other hand, in the superconductor with $U_{12}=+5t$ one gets $|\Delta_1|=0.20t$ and $|\Delta_2|=0.23t$ at the impurity site. The order parameters are suppressed a few times more strongly in the superconductor with repulsive interorbital interaction.

Similar effect has been earlier noted[38] within the weak-coupling Eilenberger theory for finite (interband) impurity concentration in the two-band superconductors. Here we observe similar behavior already for single impurity. Performing analytical studies of the $T_c$ suppression in the two-band case, the authors[38] have noted that strong suppression of superconductivity for finite concentration of interband impurities is to be expected for the interband couplings fulfilling the inequality

$$U_{12} \geq -\frac{N_1^2 U_{11} + N_2^2 U_{22}}{2N_1 N_2}. \tag{20}$$

In other words, much weaker suppression of $T_c$ is expected for attractive interband interaction (note that positive interactions are attractive in the notation of the paper[38]).

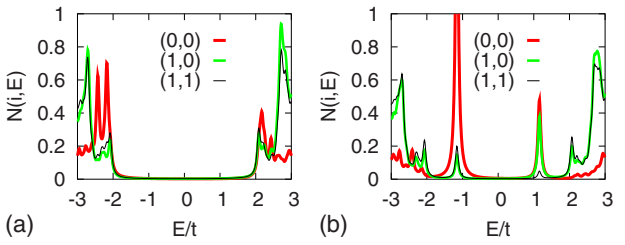


FIG. 9. (Color online) The energy dependence of the quasiparticle density of states at the interband impurity $V_{imp}(\vec{r}_i)=V_{imp}^{12}(\vec{r}_i)$ and the neighboring sites for attractive (left panel) and repulsive (right panel) interband pairing interactions.

In more detail, this feature is again illustrated in Fig. 9, which shows the energy dependence of the quasiparticle density of states at and near the impurity site for attractive (left panel) and repulsive (right panel) interorbital interactions. In the latter case the order parameter at the impurity site and around it is strongly suppressed and new states appear inside the gap. The intraorbital impurity scattering (not shown) is not as effective in suppressing superconductivity independently of the $U_{12}$ sign. This is due to a similar mechanism (Anderson theorem) to that operating in single-band $s$-wave superconductors.[39]

There is also an interesting analogy between our two-orbital model and the two-band model related to the phases of the order parameters. As noted earlier for repulsive interband interactions the $s_{\pm}$-wave pairing state[34,40] appears. This state has $s$-wavelike order parameters with the phases differing by $\pi$ on two Fermi surfaces. It means that if the phase of $\Delta_\lambda$ on one of the Fermi surfaces is $\phi$, the phase on the other

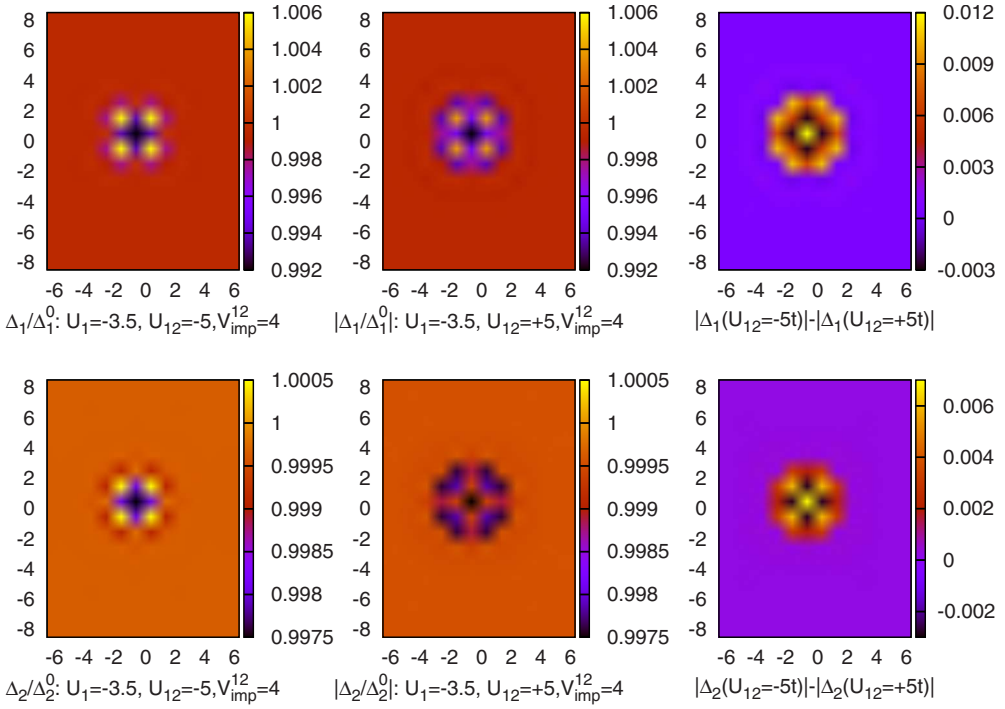


FIG. 8. (Color online) The changes in the order parameters around the interband impurity $V_{imp}^{12}$ located at the center of the superconducting cluster with $U_{11}=-3.5t$. Left panels are for $U_{12}=-5t$ and middle panels for $U_{12}=5t$. The right panels show the maps of difference between the values of the order parameter for attractive and repulsive interband interactions.

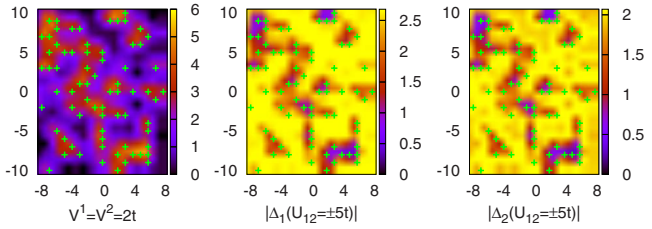


FIG. 10. (Color online) The distribution of the intraorbital impurity potential $V^1_{imp}(\vec{r}_i)=V^2_{imp}(\vec{r}_i)$ (left panel), local values of the order parameter $\Delta_1$ (middle panel) and $\Delta_2$ (right panel). These results are independent regardless the interorbital pair scattering $U_{12}=\pm 5t$ is of repulsive or attractive type.

one is $\phi+\pi$. This phase relation is, in fact, responsible for strong suppression of superconductivity by interband impurities.

In our orbital picture the phases of the gaps $\Delta_1$ and $\Delta_2$ change at the $V^{12}_{imp}$ impurity site by $\pi$ with respect to those in the bulk. Obviously, there is no such effect for attractive interorbital interaction.

## V. MANY IMPURITIES IN THE TWO-ORBITAL SUPERCONDUCTOR

In this section, we consider the two-orbital superconductor with interorbital and intraorbital impurities. Our sample is of rectangular shape. It is $L=17\times 21$ sites large with a square lattice and a unit lattice constant. It contains 20% interorbital or intraorbital impurities randomly distributed. We are not averaging over the distributions of impurities but rather calculate the local properties at each site for a given configuration of impurities and present the results in the form of maps. To make the impurities more realistic we assume that they are extended $V^{\lambda\lambda'}_{imp}(\vec{r}_i)=V^{\lambda\lambda'}f_{id}$ with $f_{id}$ being a number from the Gaussian distribution at the sites distance $id=1,\sqrt{2},2$ from the impurity. The superconductor studied in this section is characterized by one active orbital with $U_{11}=-3.5t$ and interorbital interaction $|U_{12}|=5t$. The other parameters are: $e_2-e_1=2t$, $t_1=t$, $t_2=2t$, $t_{12}=0.05$, and $n=1.2$. All energies are measured in the units of $t$.

Figures 10 and 11 show the suppression of both order parameters for intraorbital and interorbital impurities, respectively. In all cases one observes similar patterns and a large degree of (anti)correlation between the impurity positions and the gap values. However, the interorbital impurities suppress both order parameters to a lesser extent for $U_{12}=-5t$ than for the opposite sign of this coupling. For negative $U_{12}$ the phases of the two order parameters are the same and the scattering of a pair from orbital 1 into orbital 2 is "harmless," as the superconductor as a whole looks like $s$-wave one, and is protected against impurities by the Anderson theorem.[39]

Even though the maps presenting suppression of the order parameters by intraorbital and interorbital impurities shown in the Figs. 10 and 11 look largely similar big differences are observed in the local densities of states. They are shown in Figs. 12 and 13. The left panels of both figures show the local densities of states $N(1,y,E)$ as a function of energy along the line $x=-7$. The middle panels present the results

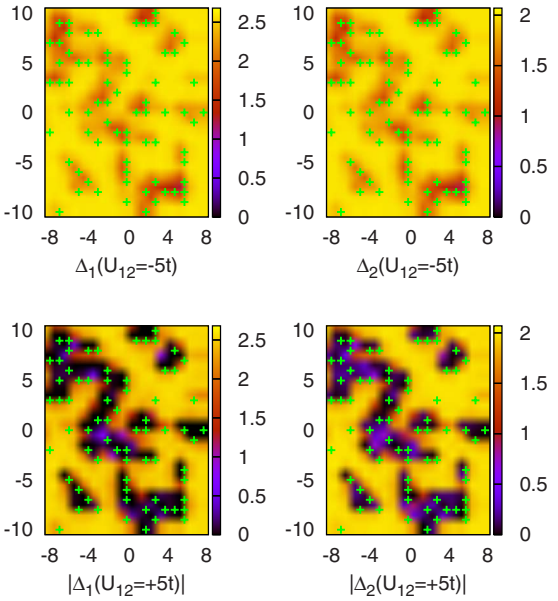


FIG. 11. (Color online) The maps of the local values of the order parameters $\Delta_1$ (left panels) and $\Delta_2$ (right panels). The upper two figures are obtained for the attractive interorbital interaction $U_{12}=-5t$, whereas lower figures show the data for repulsive $U_{12}=5t$.

for $N(2,y,E)$ and the total DOS is plotted in the right panels along the same cuts. Intraorbital impurities, Fig. 12 induce large inhomogeneities, which show up as gaps in the local density of states of the amplitude largely changing from site to site. Sites close in space may have very differentiated gaps. Similarly, the interorbital impurities in a superconductor with large attractive pair scattering also induce inhomogeneities. However, they are much smaller, at least if calculated for the same distribution and strength of impurities. The gaps also change from site to site but more gradually, i.e., on a larger spatial scale. On the contrary, the same interorbital impurities nearly completely destroy the superconductivity in the system with strongly repulsive interorbital pair scattering, i.e., in the $s_{\pm}$-like state.

Different reaction of the systems with repulsive and attractive interorbital interactions to impurities may well be characterized by the dependence of the superconducting transition temperature $T_c$ or the average gap on the strength of $V_{imp}$. In the left panel of Fig. 14 we show the relative change

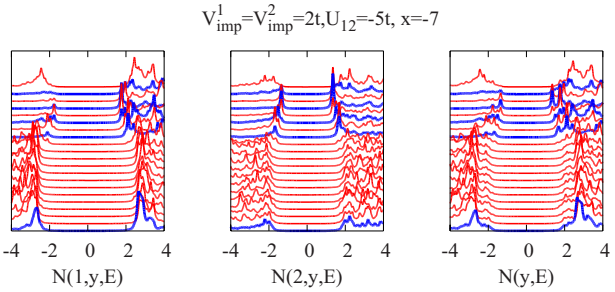


FIG. 12. (Color online) The partial (left and middle panels) and the total (right panel) densities of states as a function of energy close to the Fermi energy at the sites along the line $x=-7$ of the same sample as shown in Fig. 10.

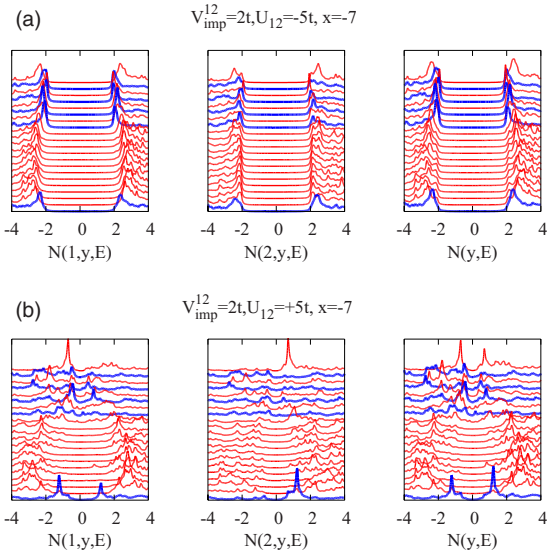


FIG. 13. (Color online) The energy dependence of the partial and total densities of states $N(\lambda, y, E)$ at the sites along the line $x=-7$ of the sample shown in Fig. 11. The upper row corresponds to attractive interorbital interactions, whereas the lower row to repulsive ones.

in $\langle \Delta_1 + \Delta_2 \rangle$ in the impure system normalized to its clean value $\langle \Delta_1 + \Delta_2 \rangle_0$ with the increasing strength of intraorbital impurities $V_{imp} = V^1_{imp} = V^2_{imp}$ (dashed curve with triangles) and interorbital impurities $V_{imp} = V^{12}_{imp}$ in a system with $U_{12} = -5t$ (curve with full squares) or $U_{12} = +5t$ (curve with dots). The right panel of that figure shows the changes in $T_c$ with $V^{12}_{imp}$ for two signs of pair scattering. In full analogy with the results of Kogan *et al.*[38] we observe much stronger diminishing of $T_c$ (normalized to its clean system value $T_{c0}$) for repulsive than for attractive $U_{12}$. Similar dependence of $T_c$ on impurity strength for both signs of $U_{12}$ at small disorder is attributed to our use of the Bogolubov-de Gennes approach which is more suitable to study inhomogeneous systems than the $\vec{k}$-space-based Elishberg or BCS theories. In the BdG approach the condensate wave function may distort around the impurity and this allows the system to keep its condensation energy and $T_c$ much higher than it would result from the Abrikosov-Gorkov approach to impure superconductors, which does not allow for local changes in the wave function.

## VI. DISCUSSION AND CONCLUSIONS

We have studied the model of two-band superconductor with interorbital pair scattering interactions. In the first part of the paper we focused on some general aspects of the two-band model. In particular, we have found that the presence of Van Hove singularity in the density of states in one of the bands is responsible for strong enhancement of the superconducting transition temperature of intraband only superconductor in the weak-coupling limit, i.e., for $\lambda_0 \ll 1$. However, neglecting the changes in the prefactor, the mere increase in effective interband coupling by Van Hove singularity seems to be not large enough to make the electron-phonon coupling responsible for superconductivity, at least so in LaFeAsO, for

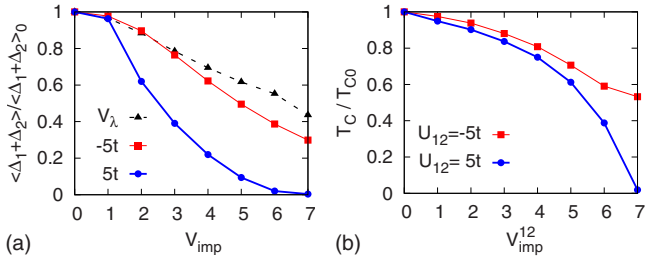


FIG. 14. (Color online) The left panel shows the dependence of the normalized average order parameter on $V_{imp} = V^1 = V^2$ (dashed curve with triangles) and on $V_{imp} = V^{12}$ with $U_{12} = -5t$ (curve with full squares) or $U_{12} = +5t$ (curve with dots). The right panel shows the changes in $T_c$ with $V^{12}$ for two signs of interorbital pair scattering.

which the coupling constant matrix has been found[41] with $\lambda_{12} = 0.093$ and $\lambda_{21} = 0.124$. Interestingly, our analysis suggests that for the elevated values of $\lambda_0 \geq 0.5$ the presence of Van Hove singularity diminishes $T_c$ in comparison to the system without logarithmic enhancement of DOS. The model with both types of pairing interactions (i.e., intraband and interband) leading to $s$- or $s_\pm$-wave symmetry displays a number of features similar to those observed in real many band materials, particularly $MgB_2$ and iron pnictides. The interband impurity scatterers were intensively studied[42] in connection with $MgB_2$. It has been found that the Eliashberg theory leads to much slower rate of $T_c$ suppression than that predicted on the basis of BCS treatment.

$MgB_2$ is a well-established superconductor with two gaps.[43] It is believed to have one active band and relatively weak interband coupling. Its much slower[44] suppression of superconducting transition temperature by impurities[45,46] than that predicted by the Abrikosov-Gorkov theory may point towards the interband character of impurities and repulsive character of interband pair scattering ($U_{12} > 0$). In the context of the two-orbital model of inhomogeneous systems similar case is illustrated in the upper row of Fig. 13.

Another prominent recent example of many band superconductors is provided by the iron pnictides.[47] These superconductors seem to belong to another class of many band materials in which the interband interaction is dominant and the order parameter has different signs on two Fermi-surface sheets[34]—the $s_\pm$ state.

The existing samples are certainly strongly disordered, as it can be inferred from large values of resistance just above $T_c$ and the usual $\vec{k}$-space description is not valid. That is why we have adopted here the orbital description which remains valid in the real-space representation. Despite large disorder the pnictides are superconducting with quite large $T_c$. This suggests $s$- or $s_\pm$-wavelike order parameter. As we have seen the superconductor with dominant attractive $U_{12}$ interactions is quite robust against impurities, both of intraorbital and (even more) interorbital types (cf. Figs. 12 and 13).

The robustness of the two-orbital superconductors with attractive interorbital pair scattering to the impurities can be traced back to the Anderson theorem. On the other hand, the $s_\pm$-like state existing in systems with repulsive interorbital pair interactions is sensitive to interorbital impurity scatter-

ing. These results are real-space analogs to the previous findings reported for similar calculations in reciprocal space.[38,42]

The maps plotted in Figs. 10 and 11 are in qualitative agreement with the recent scanning tunneling microscopy (STM) studies for pnictide superconductors.[48–50] In those papers a relatively small variation in local gaps have been observed with the average gap $\bar{\Delta}=6-7$ meV and $2\Delta(0)/k_BT_c \approx 7$ indicating strong-coupling superconductivity. The detailed analysis of the STM spectra of pnictides will be the subject of future studies.

## ACKNOWLEDGMENT

This work has been partially supported by the Ministry of Science and Education under the Grant No. N N202 1698 36.

*karol@tytan.umcs.lublin.pl

[1] H. Suhl, B. T. Matthias, and L. R. Walker, Phys. Rev. Lett. **3**, 552 (1959).
[2] V. A. Moskalenko, Fiz. Met. Metalloved. **8**, 503 (1959).
[3] M. Suffczynski, Phys. Rev. **128**, 1538 (1962).
[4] J. Kondo, Prog. Theor. Phys. **29**, 1 (1963).
[5] J. G. Bednorz and K. A. Müller, Z. Phys. B: Condens. Matter **64**, 189 (1986); K. A. Müller and J. G. Bednorz, Science **237**, 1133 (1987).
[6] Y. Maeno, H. Hashimoto, K. Yoshida, S. Nishizaki, T. Fujita, J. G. Bednorz, and F. Lichtenberg, Nature (London) **372**, 532 (1994).
[7] J. Nagamatsu, N. Nakagawa, T. Muranaka, Y. Zenitani, and J. Akimitsu, Nature (London) **410**, 63 (2001).
[8] Y. Kamihara, H. Hiramatsu, M. Hirano, R. Kawamura, H. Yanagi, T. Kamiya, and H. Hosono, J. Am. Chem. Soc. **128**, 10012 (2006).
[9] Y. Kamihara, T. Watanabe, M. Hirano, and H. Hosono, J. Am. Chem. Soc. **130**, 3296 (2008).
[10] Y. Wang, T. Plackowski, and A. Junod, Physica C **355**, 179 (2001); F. Bouquet, Y. Wang, I. Sheikin, T. Plackowski, A. Junod, S. Lee, and S. Tajima, Phys. Rev. Lett. **89**, 257001 (2002).
[11] M. Angst, R. Puźniak, A. Wiśniewski, J. Jun, S. M. Kazakov, J. Karpiński, J. Roos, and H. Keller, Phys. Rev. Lett. **88**, 167004 (2002).
[12] A. P. Mackenzie and Y. Maeno, Rev. Mod. Phys. **75**, 657 (2003).
[13] K. I. Wysokiński, G. Litak, J. F. Annett, and B. L. Györffy, Phys. Status Solidi B **236**, 325 (2003).
[14] I. I. Mazin and J. Schmalian, Physica C **469**, 614 (2009).
[15] M. V. Sadovskii, Phys. Usp. **51**, 1201 (2008).
[16] A. L. Ivanovskii, Phys. Usp. **51**, 1229 (2008).
[17] Yu. A. Izyumov and E. Z. Kurmaev, Phys. Usp. **51**, 1261 (2008).
[18] H. Ding, P. Richard, K. Nakayama, T. Sugawara, T. Arakane, Y. Sekiba, A. Takayama, S. Souma, T. Sato, T. Takahashi, Z. Wang, X. Dai, Z. Fang, G. F. Chen, J. L. Luo, and N. L. Wang, EPL **83**, 47001 (2008).
[19] A. V. Chubukov, D. V. Efremov, and I. Eremin, Phys. Rev. B **78**, 134512 (2008).
[20] K. Kuroki, S. Onari, R. Arita, H. Usui, Y. Tanaka, H. Kontani, and H. Aoki, Phys. Rev. Lett. **101**, 087004 (2008).
[21] S. Raghu, X.-L. Qi, C.-X. Liu, D. J. Scalapino, and S.-C. Zhang, Phys. Rev. B **77**, 220503(R) (2008).
[22] W. V. Liu and F. Wilczek, Phys. Rev. Lett. **90**, 047002 (2003).
[23] L. Fanfarillo, L. Benfatto, S. Caprara, C. Castellani, and M. Grilli, Phys. Rev. B **79**, 172508 (2009).
[24] M. S. Laad and L. Craco, Phys. Rev. Lett. **103**, 017002 (2009).
[25] A. Y. Liu, I. I. Mazin, and J. Kortus, Phys. Rev. Lett. **87**, 087005 (2001).
[26] We start with the two-orbital description of the system and consider the single- and two-particle (in the spin-singlet Cooper channel) scattering between orbitals.
[27] T. Örd and N. Kristofell, Physica C **331**, 13 (2000).
[28] O. V. Dolgov, I. I. Mazin, D. Parker, and A. A. Golubov, Phys. Rev. B **79**, 060502(R) (2009).
[29] N. N. Bogoljubov, V. V. Tolmachev, and D. V. Shirkov, Fortschr. Phys. **6**, 605 (1958).
[30] J. G. Valatin, Nuovo Cimento **7**, 843 (1958).
[31] J. B. Ketterson and S. N. Song, *Superconductivity* (Cambridge University Press, Cambridge, 1999).
[32] K. I. Wysokinski, J. F. Annett, and B. L. Györffy, Supercond. Sci. Technol. **22**, 014009 (2009).
[33] A. Bussmann-Holder, R. Micnas, and A. R. Bishop, Eur. Phys. J. B **37**, 345 (2004).
[34] I. I. Mazin, D. J. Singh, M. D. Johannes, and M. H. Du, Phys. Rev. Lett. **101**, 057003 (2008).
[35] Y. Bang and H.-Y. Choi, Phys. Rev. B **78**, 134523 (2008).
[36] R. S. Markiewicz, J. Phys. Chem. Solids **58**, 1179 (1997).
[37] J. Labbe and J. Bok, Europhys. Lett. **3**, 1225 (1987).
[38] V. G. Kogan, C. Martin, and R. Prozorov, Phys. Rev. B **80**, 014507 (2009).
[39] P. W. Anderson, J. Phys. Chem. Solids **11**, 26 (1959).
[40] K. Seo, B. A. Bernevig, and J. Hu, Phys. Rev. Lett. **101**, 206404 (2008).
[41] L. Boeri, O. V. Dolgov, and A. A. Golubov, Physica C **469**, 628 (2009).
[42] B. Mitrović, J. Phys.: Condens. Matter **16**, 9013 (2004).
[43] J. Kortus, Physica C **456**, 54 (2007); K. Rogacki, B. Batlogg, J. Karpinski, N. D. Zhigadlo, G. Schuck, S. M. Kazakov, P. Wägli, R. Puźniak, A. Wiśniewski, F. Carbone, A. Brinkman, and D. van der Marel, Phys. Rev. B **73**, 174520 (2006).
[44] A. A. Golubov and I. I. Mazin, Phys. Rev. B **55**, 15146 (1997).
[45] M. R. Eskildsen, M. Kugler, S. Tanaka, J. Jun, S. M. Kazakov, J. Karpinski, and O. Fischer, Phys. Rev. Lett. **89**, 187003 (2002).
[46] S. M. Kazakov, R. Puzniak, K. Rogacki, A. V. Mironov, N. D. Zhigadlo, J. Jun, Ch. Soltmann, B. Batlogg, and J. Karpinski, Phys. Rev. B **71**, 024533 (2005).
[47] K. Ishida, Y. Nakai, and H. Hosono, J. Phys. Soc. Jpn. **78**, 062001 (2009).
[48] Y. Yin, M. Zech, T. L. Williams, X. F. Wang, G. Wu, X. H. Chen, and J. E. Hoffman, Phys. Rev. Lett. **102**, 097002 (2009).
[49] F. Massee, Y. Huang, R. Huisman, S. de Jong, J. B. Goedkoop, and M. S. Golden, Phys. Rev. B **79**, 220517(R) (2009).
[50] Y. Yin, M. Zech, T. L. Williams, and J. E. Hoffman, Physica C **469**, 535 (2009).